Hyperfine Interactions **135:** 191–213, 2001.

A New Way of Looking at Nuclear Resonant Scattering ⋆

GILBERT R. HOY

Physics Department, Old Dominion University, Norfolk, VA 23529-0116, USA

Abstract. A new model for nuclear-resonant scattering of gamma radiation from resonant matter has been developed and is summarized here. This "coherent-path" model has lead to closed-form, finite-sum solutions for radiation scattered in the forward direction. The solution provides a unified microscopic picture of nuclear-resonant scattering processes. The resonant absorber or scatterer is modeled as a one-dimensional chain of "effective" nuclei or "effective" planes. The solution is interpreted as showing that the resonant radiation undergoes sequential scattering from one absorber "nucleus" or "plane" to another before reaching the detector. For recoil-free processes the various "paths" to the detector contribute coherently. The solution for this case gives calculated results that are indistinguishable from those using the classical optical model approach, although the forms of the solutions are completely different. The coherent-path model shows that the "speed-up" and "dynamical beating" effects are primarily a consequence of the fact that the single "effective" nuclear scattering processes are 180° out of phase with the incident radiation while the double nuclear scattering processes are in phase with the incident radiation. All multiple scattering paths are, and must be, included. The model can also treat the incoherent processes, i.e., processes involving gamma emission with recoil or conversion-electron emission. The source of the resonant gamma radiation can be from a radioactive source or from synchrotron radiation: both cases are treated. The model is used to explain and understand the results when each of the following experimental procedures is applied: time-differential Mössbauer spectroscopy, time-differential synchrotron radiation spectroscopy, enhanced-resolution resonant-detector Mössbauer spectroscopy, and the "gamma echo".

Key words: nuclear resonant scattering, Mössbauer spectroscopy, gamma echo.

1. Introduction

In recent years a new model for nuclear resonant scattering has been developed. As the model evolved, the resulting solutions gave rise to a change in the name of the model. It is now called the "coherent-path model", because the form of the solution consists of a summation over the various "paths" that the gamma radiation takes to reach the detector. The model has been applied successfully to various experimental and theoretical problems. These include; time differential Mössbauer spectroscopy (TDMS), time differential synchrotron radiation spectroscopy, enhanced-resolution resonant-detector Mössbauer spectroscopy, and the "gamma echo" effect. In this paper the results of the model will be reviewed and summarized. The paper is divided into several sections. Each section deals with one

⋆ This paper is dedicated to Professor Dr. Romain Coussement.

of the particular topics noted above. The first section outlines the general approach and treats the radioactive source case.

2. The general approach: the radioactive source case

The Mössbauer effect [1, 2] is due to the recoil-free emission and/or recoil-free absorption of gamma radiation that can happen in solids. The experimental technique that the coherent-path model addresses in this section has been called time-differential Mössbauer spectroscopy (TDMS) [3]. In this method a "lifetime curve" of the first excited state in the source is obtained as done in nuclear physics but, in this case, the resonant radiation must pass through a resonant absorber before reaching the detector. The resulting "lifetime curve" does not show the expected exponential behavior. This effect has been called "time filtering". Hamermesh [3] analyzed the recoil-free process using a classical optical model. Subsequently, Harris [4], using methods developed by Heitler [5], was able to show that the quantum mechanical treatment gives the same result. Using the same mathematical methods as Heitler and Harris, with the added features that the resonant absorber is represented as a one-dimensional chain of N "effective" nuclei and only the resonant radiation scattered in the forward direction is considered, allowed development of the coherent-path model [6]. However, the model is deceptive. It only appears to be one-dimensional. It actually treats the sample as a series of N "effective" planes. A closed-form solution is found whose appearance is different from the classical optical and other quantum mechanical solutions.

The problem addressed, in this section, is the one in which a radioactive source nucleus emits gamma radiation and this radiation interacts with a polycrystalline absorber containing resonant nuclei, which are initially in the ground state. The time at which the source nucleus is in its first excited state is determined by a precursor gamma ray and sets the time $t = 0$. The coherent-path model predicts the shape of the lifetime curve, i.e., the time-dependent intensity of radiation from that state, when the radiation passes through nuclear-resonant matter.

The general method used in developing the new model is discussed in Harris [4], Heitler [5] and [6]. The method applies quantum mechanical time-dependent theory in the frequency domain to obtain a set of coupled linear algebraic equations. The Hamiltonian of the system is divided into two parts; H_0 corresponding, in this case, to the nuclear states and the free radiation field, taken as plane waves, and H which is responsible for making transitions between the states $|\phi_p\rangle$ of H_0 by allowing the nuclei to absorb and emit radiation. The state of the system $|\psi(t)\rangle$ can be expressed as

$$|\psi(t)\rangle = \sum_p a_p(t)\, \mathrm{e}^{-\mathrm{i}(E_p t/\hbar)} |\phi(0)\rangle, \tag{1}$$

where $|\phi_p(0)\rangle$ is an eigenstate of H_0. Solving the Schrödinger equation in the usual way, one arrives at a set of coupled differential equations relating the expansion coefficients $a_p(t)$.

$$\mathrm{i}\hbar\frac{\mathrm{d}a_p}{\mathrm{d}t} = \sum_m a_m(t)\,\mathrm{e}^{\mathrm{i}(\omega_p-\omega_m)t}\langle\phi_p(0)|H|\phi_m(0)\rangle + \mathrm{i}\hbar\delta_{pl}\delta(t). \tag{2}$$

The Kronecker delta and the delta function on the right-hand side in Equation (2) are needed to denote that at time $t = 0$ the system is in the state where $p = l$ (i.e., for our case only the source nucleus is excited).

Now introducing the Fourier transform

$$a_p(t) = -\frac{1}{2\pi\,\mathrm{i}}\int_{-\infty}^{\infty}\mathrm{d}\omega A_p(\omega)\,\mathrm{e}^{\mathrm{i}(\omega_p-\omega)t} \tag{3}$$

into Equation (2) and writing $\delta(t)$ in an integral representation gives,

$$(\omega-\omega_p)A_p(\omega) = \sum_m A_m(\omega)\frac{\langle\phi_p(0)|H|\phi_m(0)\rangle}{\hbar} + \delta_{pl}. \tag{4}$$

However, in order for $a_p(t) = 0$ for all p when $t < 0$, $A_p(\omega)$ must have a pole only in the lower half of the complex plane. To ensure this, Equation (4) is re-written

$$(\omega-\omega_p+\mathrm{i}\varepsilon)A_p(\omega) = \sum_m A_m(\omega)\frac{\langle\phi_p(0)|H|\phi_m(0)\rangle}{\hbar} + \delta_{pl}, \tag{5}$$

where $\varepsilon > 0$. This formalism is now applied to study the problem where at $t = 0$ there is an excited source nucleus, and N resonant "absorber" nuclei, in the ground state, located between the source and the detector.

For this case there are five amplitudes: $A(\omega)$ the source nucleus located at the origin is excited (energy $\hbar\omega_0$), all absorber nuclei are in the ground state, and no photons or conversion electrons are present; $B_k(\omega)$ all nuclei are in the ground state and a photon is present of wave number k and energy $\hbar\omega_k$; $C_m(\omega)$ only the absorber nucleus located at $x = x_m$ is excited (energy $\hbar\omega_0'$) and no photons or conversion electrons are present; $D_p(\omega)$ a conversion electron from the source nucleus is present having momentum p, all nuclei are in the ground state; and $E_{mp}(\omega)$ a conversion electron is present from the absorber nucleus located at $x = x_m$, and all nuclei are in the ground state. The photon polarization and the electron spin are neglected because including these factors would only obscure the relatively simple form of the final solution. Assuming that at time $t = 0$ the source nucleus is excited, and substituting these amplitudes into Equation (5) gives the following set of coupled linear equations,

$$(\omega-\omega_0+\mathrm{i}\varepsilon)A(\omega) = 1 + \sum_k\frac{B_k(\omega)H_k}{\hbar} + \sum_p\frac{D_p(\omega)H_p}{\hbar}, \tag{6}$$

$$(\omega-\omega_k+\mathrm{i}\varepsilon)B_k(\omega) = \frac{A(\omega)H_k^*}{\hbar} + \sum_m\frac{C_m(\omega)H_k^*}{\hbar}\mathrm{e}^{-\mathrm{i}kx_m}, \tag{7}$$

$$(\omega - \omega_0' + \mathrm{i}\varepsilon)C_m(\omega) = \sum_k \frac{B_k(\omega)H_k}{\hbar}\mathrm{e}^{\mathrm{i}kx_m} + \sum_p \frac{E_{mp}(\omega)H_p}{\hbar}\mathrm{e}^{\mathrm{i}(p/\hbar)x_m}, \tag{8}$$

$$(\omega - \omega_p + \mathrm{i}\varepsilon)D_p(\omega) = \frac{A(\omega)H_p^*}{\hbar}, \tag{9}$$

$$(\omega - \omega_p + \mathrm{i}\varepsilon)E_{mp}(\omega) = \frac{C_m(\omega)H_p^*}{\hbar}\mathrm{e}^{-\mathrm{i}(p/\hbar)x_m}, \tag{10}$$

where H_k and H_k^* are the matrix elements corresponding to absorption and emission of a photon, respectively. Also H_p and H_p^* are the matrix elements corresponding to absorption and emission of a conversion electron, respectively.

The meaning of these equations can be made clear by considering, for example, Equations (6) and (7). Equation (6) governs the amplitude for finding the source nucleus excited, $A(\omega)$. Since this is the case at $t = 0$, that accounts for the "1" on the right-hand side. The source can also get to the excited state, when in the ground state, by absorbing a photon that is present. This is the meaning of the second term on the right-hand side. Similarly, when the source nucleus is in the ground state, it can be excited by absorbing its own conversion electron. Since the source nucleus is at the origin of our coordinates, there are no spatial phase factors needed. On the other hand consider Equation (7). This is the equation describing the situation in which all nuclei are in the ground state and there is only a photon present, $B_k(\omega)$. How can this happen? The source can emit a photon; that is the meaning of the first term on the right-hand side. Also one absorber nucleus, located at x_m, can emit a photon. Now one must put in the phase factor, representing the fact that this photon appears at $x = x_m$. Furthermore, one must allow any other absorber nucleus to do the same thing: the summation over all absorber nuclei is needed. The other three equations can be understood in the same way. The solution to the problem is obtained by solving this set of coupled linear equations. This problem is treated and solved in [6].

The amplitude corresponding to the resonant gamma radiation being transmitted through the absorber to the detector, when the source and absorber nuclei are in exact resonance, is given by

$$\psi_r(t') = \psi_r^{\text{source}}(t')\left[1 + \sum_{n=1}^{N}\binom{N}{n}\left(-\frac{\Gamma_r t'}{2\hbar}\right)^n \frac{1}{n!}\right], \tag{11}$$

where $\psi_r^{\text{source}}(t')$ is due to the source alone, Γ_r is the radiative width, and t' is the time measured from the time of formation of the first excited nuclear level in the source. The right-hand side of Equation (11) contains all the amplitudes contributing to the total forward scattering amplitude. This solution can be understood by identifying the various contributing amplitudes. First, there is the amplitude corresponding to the probability amplitude that the source radiation reaches the detector

without interacting with any absorber nuclei. This is the first term on the right-hand side. There is another amplitude for the "path" in which the source radiation is absorbed and re-emitted by one absorber nucleus before reaching the detector. This single scattering process is termed the "one-hop" process. This amplitude contributes N times since there are N absorber nuclei. This amplitude is the first term involving the summation sign. There is another amplitude or "path" where the source radiation makes two "hops" (double scattering) on absorber nuclei before reaching the detector. This amplitude can occur according to the number of ways two objects can be selected from N objects, i.e., the binomial coefficient N over 2: the second term under the summation sign. The other "paths" involving more hops (multiple scattering) are of a similar nature. It is important to take note that for each hop (single scattering) there is an 180° phase shift, the minus sign, and a probability given by the radiative width $\Gamma_r/2$.

In the model the resonant gamma radiation is treated as a plane wave, and the phase shift of the forward-scattered radiation due to a single "effective" nucleus is found to be π, as noted by the minus sign in Equation (11) above. In X-ray diffraction it is well known that a single resonant scattering gives a $\pi/2$ phase shift and a further $\pi/2$ phase shift arises when a summation is made over the whole plane of resonant scatterers. Noticing that the model gives such a π phase shift, when scattering off a single "effective" nucleus, as seen by the minus sign in Equation (11), suggests that the theory more appropriately corresponds to a nuclear resonant sample represented by N "effective" parallel planes or slices. This realization helps explain why the model works so well.

To summarize, one can say that the source emits recoil-free radiation and, when the absorber nuclei do the same, it is impossible to distinguish which "path" was taken for each photon that reaches the detector. Therefore, all paths must be added coherently. Thus to obtain the time-dependent intensity of gamma radiation reaching the detector, all the contributing amplitudes must be added before taking the absolute value squared. The only modification needed in adapting Equation (11) to this case is to realize that the probability for recoil-free gamma-ray absorption or emission is not given by the radiative width Γ_r alone. Now the radiative width must be multiplied by the recoil-free fraction (f). The time-dependent intensity of radiation reaching the detector when the source nucleus and absorber nuclei are in resonance is given by modifying Equation (11) accordingly. The result is

$$I_{fr}(t') = \frac{f\Gamma_r}{2\hbar} e^{-(\Gamma/\hbar)t'} \left[1 + \sum_{n=1}^{N} \binom{N}{n} \left(\frac{-f\Gamma_r t'}{2\hbar} \right)^n \frac{1}{n!} \right]^2, \tag{12}$$

where Γ is the total decay width. Using Equation (12), one can see "speed-up" and "dynamical beat" effects familiar [3, 7] from experimental results and the classical optical model. It appears that the source nucleus is initially decaying more rapidly than normal, i.e., the speed-up effect. Also the time-dependent intensity using thick absorbers shows local maxima at times different from zero, i.e., dynamical beats.

In this coherent-path model the explanation of the speed-up and the dynamical beat effects can be seen by looking at the phase of each contributing amplitude in Equation (12). It is the factors inside the square brackets of Equation (12) that need to be studied. Each term, corresponding to a particular value of n, contributes an "n-hop path" amplitude. The number N, the effective "thickness" of the "absorber", determines the total number of different n-hop processes.

It is interesting to point out that the calculated results using the coherent-path model are identical to those obtained using the classical optical model when N is correlated with the usual nuclear-resonant thickness parameter β. The thickness parameter β is equal to $N_0 f \sigma_0 d$, where N_0 is the number of resonant nuclei/cm^3 f is the recoil-free fraction, σ_0 is the maximum cross section evaluated on resonance, and d is the thickness of the sample. This agreement is shown in Figure 1.

To understand the coherent-path model results, consider an iron "absorber" whose resonant thickness can be correlated with $N = 50$, as shown in Figure 1. In this case we will have 50 one-hop processes, 1,225 two-hop processes... up to and including one 50-hop process where all absorber nuclei participate. An informative way to show the various contributions is to plot each individual term in the sum, i.e., the result for each "n" multiplied, for convenience, by the exponential function. Figure 2 shows the no-hop, the one-hop, and the two-hop amplitudes each multiplied by the exponential factor for the case when the absorber contains $N = 50$ effective nuclei. Notice that the one-hop amplitude is 180° out of phase with respect to the no-hop and the two-hop amplitudes. When these amplitudes are added and then squared, the one-hop amplitude causes the resulting curve to decay more rapidly near $t = 0$, the speed-up effect. At later times the contribution from

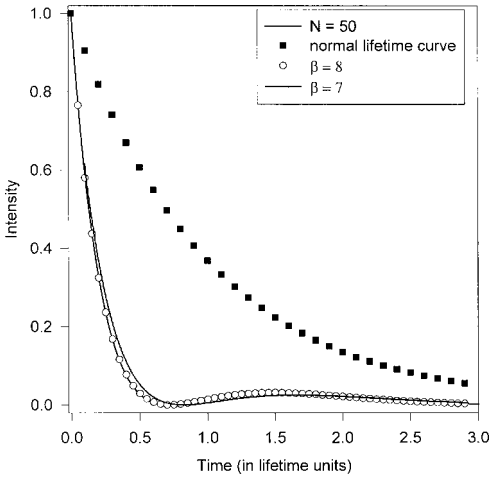

Figure 1. A comparison of the coherent-path model with the classical optical model assuming recoil-free processes for ^{57}Fe. The model with $N = 50$ agrees with the classical optical model for $\beta = 8$. The result for $\beta = 7$ does not agree. The result for $\beta = 9$ does not agree either, but this is not shown to keep the figure legible. Notice the speed-up effect and dynamical beat.

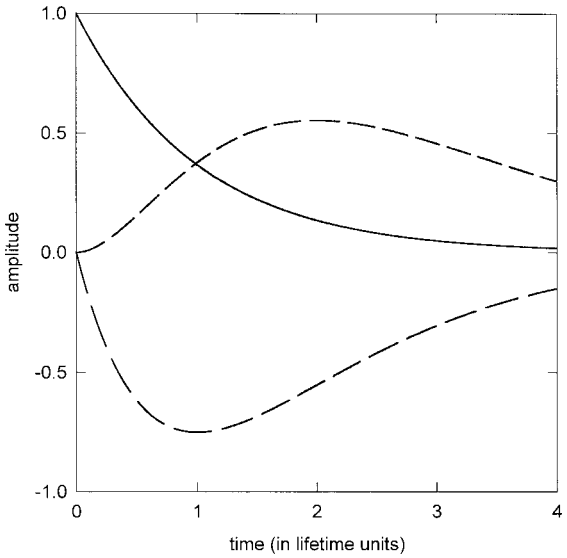

Figure 2. The "amplitudes" (see the text for explanation) for the no-hop (solid line), one-hop (longer dashed line), and two-hop (shorter dashed line) multiple scattering processes are shown multiplied by the decaying exponential. The case chosen is for $N = 50$. Notice that the one-hop amplitude is negative, while the no-hop and two-hop amplitudes are both positive. For coherent processes one must add amplitudes before squaring to obtain an intensity.

the two-hop processes helps produce the local maximum near time $t = 1.5\tau$ (τ is the natural lifetime of the first-excited state) seen in Figure 1. The exact result must be computed by considering all such "paths".

Reference [6] contains a complete treatment of the problem. In particular, the off-resonance result is given, as well as the results for the so-called incoherent processes such as emission with recoil and conversion-electron emission. In the next section a similar problem is treated, but now the source of the resonant radiation is from a synchrotron.

3. Synchrotron radiation as a source

Since 1985, when the first unambiguous observation of nuclear-resonant excitation of nuclei using synchrotron radiation (SR) [8] was achieved, there has been significant progress made in this field. A review [9] of this subject area contains a summary of experimental results, as well as many references to the original important papers in the field.

When applying the coherent-path model to this case, several modifications need to be made. In the first place, one needs to determine the relevant amplitudes. Now, at time $t = 0$ the synchrotron radiation is present and all absorber nuclei are in the ground state. This condition is given an amplitude $A_k(\omega) = A$, i.e., a constant having the dimensions of seconds. The frequency dependence of the synchrotron

radiation is taken as constant because the synchrotron radiation pulse is essentially a delta function in time for the cases we treat here. The amplitude corresponding to excitation of the mth absorber nucleus located at x_m to one of its excited states $\hbar\omega_j$ and no photons or conversion electrons present is $B_{m,j}(\omega)$. At this stage of the analysis just one excited state is considered. This means that quantum beats are not yet considered. It will become clear, later, how quantum beats can be included in the model. Another amplitude $C_{k'}(\omega)$ corresponds to the situation when all absorber nuclei are in the ground state, there are no conversion electrons, and a non-SR-pulse photon is present. The final amplitude $D_{m,p}(\omega)$ corresponds to the presence of a conversion electron from the mth nucleus, all absorber nuclei in their ground state and no photons are present. The coupled equations relating these amplitudes in one dimension are

$$A_k(\omega) = A, \tag{13}$$

$$\begin{aligned}(\omega - \omega_j + \mathrm{i}\varepsilon)B_{m,j}(\omega) \;=\; & A\sum_k \frac{H_{k,j}}{\hbar}\mathrm{e}^{\mathrm{i}kx_m} + \sum_{k'} C_{k'}(\omega)\frac{H_{k',j}}{\hbar}\mathrm{e}^{\mathrm{i}k'x_m} \\ & + \sum_p D_{m,p}\frac{H_p}{\hbar}\mathrm{e}^{\mathrm{i}(px_m/\hbar)},\end{aligned} \tag{14}$$

$$(\omega - \omega_{k'} + \mathrm{i}\varepsilon)C_{k'}(\omega) = \sum_m B_{m,j}(\omega)\frac{H^*_{k',j}}{\hbar}\mathrm{e}^{-\mathrm{i}k'x_m}, \tag{15}$$

$$(\omega - \omega_p + \mathrm{i}\varepsilon)D_{m,p}(\omega) = B_{m,j}(\omega)\frac{H^*_p}{\hbar} + \mathrm{e}^{-\mathrm{i}(px_m/\hbar)}, \tag{16}$$

where $H_{k,j}$ corresponds to absorption and $H^*_{k,j}$ corresponds to emission of a photon in the jth transition, and a similar notation is used for the conversion electron.

Solving this set of linear coupled equations gives the result for the scattered intensity in the forward direction

$$I(z,t') = \frac{\pi\Gamma_r^2}{2\hbar^2\Delta\omega_p}\mathrm{e}^{-\Gamma t'/\hbar}\left|N + \sum_{n=1}^{N-1}\left(\frac{-\Gamma_r}{2\hbar}\right)^n\binom{N}{n+1}\frac{t'^n}{n!}\right|^2. \tag{17}$$

Here $\Delta\omega_p$ is the effective bandwidth of the synchrotron radiation pulse.

If one is considering a recoil-free process, then Γ_r in Equation (17) must be multiplied by the recoil-free fraction f. Again each term in the sum, contained in the square brackets of Equation (17), corresponds to a particular hopping sequence or "path" the radiation takes to reach the detector. If we consider only the recoil-free processes, i.e., the Mössbauer effect in which radiation is absorbed and re-emitted by the nuclei without recoil, it is impossible to determine which path was

taken for each count recorded in the detector. Therefore, each path of this recoil-free type must be considered as coherent with all other such paths. The result is then

$$I(z,t') = \frac{\pi f^2 \Gamma_r^2}{2\hbar^2 \Delta\omega_p} e^{-\Gamma t'/\hbar} \left| N + \sum_{n=1}^{N-1} \left(\frac{-f\Gamma_r}{2\hbar} \right)^n \binom{N}{n+1} \frac{t'^n}{n!} \right|^2 . \tag{18}$$

There are several parameters in Equation (18); the recoil-free fraction (f), the radiative width (Γ_r), and the effective number of resonant nuclei (planes) in the sample (N). This number N is associated with the thickness of the resonant medium since it is related to the length of the one-dimensional chain of effective nuclei, or alternatively, the number of stacked effective planes. N is the only unspecified parameter in the expression for the intensity.

Using Equation (18) model-calculations are presented in Figure 3 for the case of ^{57}Fe. The calculations have been normalized to one at time $t' = 0$. Actually the value of the forward scattered intensity at $t' = 0$ is proportional to the thickness squared (N^2). The results in Figure 3 show the effect of increasing the thickness of the resonant medium. Notice the experimentally observed "speed-up" effect where the intensity radiated in the forward direction decays faster than one would expect according to the lifetime of an isolated nucleus. This effective lifetime (of the exciton in other theories [10–18]) decreases as the sample thickness increases. In fact, when the sample reaches a certain thickness, the decay curve exhibits a local maximum at a time greater than zero. This effect has been termed "dynamical beating" [7]. To see this more clearly, the lower portion of Figure 3 shows the results on an expanded scale. In principle, as the sample becomes even thicker, more local maxima appear in the time-dependent intensity curve. These results agree with those found earlier, both theoretically [18] and experimentally [19, 20]. The advantage of the new approach is that it gives new insights into the origin of the speed-up and dynamical beating effects.

To treat quantum beats we need to consider situations in which the nuclei emit radiation from recoil-free transitions at two or more frequencies that have the same polarization. Under such conditions these frequencies will interfere producing quantum beats in the time-dependent forward-scattering intensity [7, 20–22]. Of course polarization of the incident synchrotron radiation, as well as the polarization of the emitted radiation must be considered. Ψ_j corresponds to the amplitude for emitting radiation at frequency ω_j. If two or more transitions emit radiation in recoil-free processes at different frequencies having the same polarization, these amplitudes must be added due to their coherence before the intensity is calculated. This leads to the well-known phenomena of quantum beats.

The counting rate at the detector assuming that all paths are coherent is given by,

$$I(z,t') = c \left| \sum_j \Psi_j(z,t') \right|^2 , \tag{19}$$

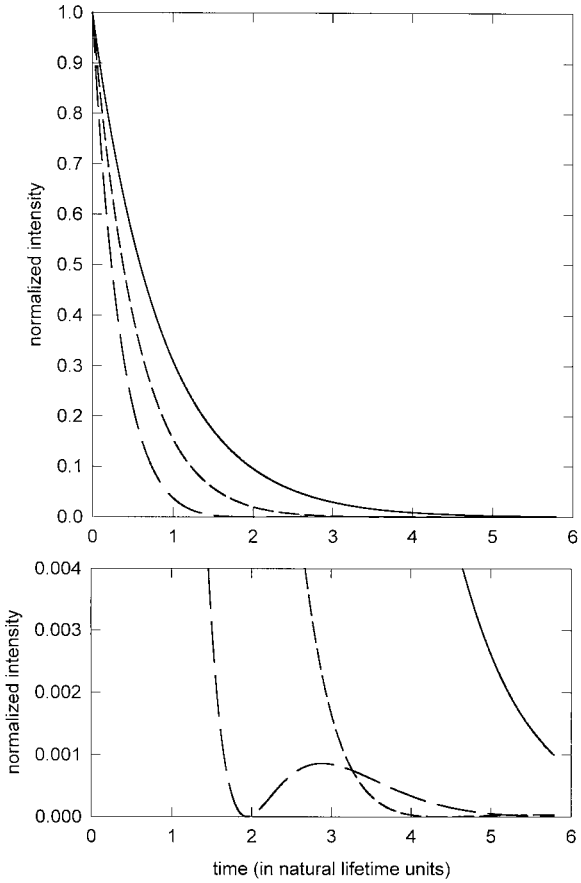

Figure 3. The time-dependent forward scattering intensity for three different values of the sample thickness, i.e., effective number of resonant nuclei $N = 5$ (solid line), 20 (shorter dashed line), and 45 (longer dashed line), is shown. Time is measured in units of the natural lifetime. Notice the "speed-up" effect and, in the lower portion of the figure, the "dynamical beat". The intensity for each case is normalized to 1 at time $t' = 0$.

where the sum over j is taken for those transitions that produce radiation having the same polarization. Modifying Equations (18) and (19) accordingly gives

$$I(z,t') = \frac{\pi\gamma_R^2}{2\hbar^2\Delta\omega_p}\left|\sum_j f_j \mathrm{e}^{-\mathrm{i}(\omega_j - \mathrm{i}\Gamma/(2\hbar))t'} \times \left[N + \sum_{n=1}^{N-1}\left(\frac{-f_j\gamma_R}{2\hbar}\right)^n \binom{N}{n+1}\frac{t'^n}{n!}\right]\right|^2, \tag{20}$$

where an f_j has been inserted to account for the specific transition probability.

In order to be specific, consider the synchrotron radiation interacting with an iron foil that is polarized so that the internal magnetic field is in the same direction

as the synchrotron beam. The synchrotron radiation is almost completely linearly polarized in the plane of the synchrotron ring. This polarization can be expressed in terms of a superposition of right and left circularly polarized states. For the case under discussion the emitted radiation is composed of only right and left circularly polarized components also. If one labels the transitions from 1 to 6 according to their increasing frequencies ω_i ($i = 1$–6), then line 1 and line 4 will have one polarization while line 3 and line 6 will have the other. Assuming no electric-field gradient at the sites of the ^{57}Fe nuclei, the difference in each pair of frequencies is the same. Thus there will be only one beat frequency corresponding to about 14 ns appearing in the time-dependent intensity spectrum. As mentioned above, one needs to incorporate the transition probability for each transition considered. In this case it is well known that lines 1 and 6 have relative intensities of 0.75 and lines 3 and 4 have relative intensities of 0.25. The resulting time-dependent forward scattering intensity is then given by Equation (20) specialized for this case

$$I(t') = \frac{\pi\Gamma_r^2}{2\hbar^2\Delta\omega_p}\left|\frac{3f}{8}\mathrm{e}^{-\mathrm{i}(\omega_1-\mathrm{i}\Gamma/(2\hbar))t'}\sum_{n=0}^{N-1}\binom{N}{n+1}\left(\frac{3f\Gamma_r t'}{8\hbar}\right)^n\frac{(-1)^n}{n!}\right.$$
$$\left.+\frac{f}{8}\mathrm{e}^{-\mathrm{i}(\omega_4-\mathrm{i}\Gamma/(2\hbar))t'}\sum_{n=0}^{N-1}\binom{N}{n+1}\left(\frac{f\Gamma_r t'}{8\hbar}\right)^n\frac{(-1)^n}{n!}\right|^2. \tag{21}$$

Figure 4 gives an example of the quantum-beat effect. In Figure 4 the result is calculated for the case when $N = 45$. This result agrees precisely with that obtained using the classical optical model [23]. The time dependence of the forward-scattered intensity is complicated here because of the combination of effects due to quantum beats (the factors $\mathrm{e}^{\pm\mathrm{i}(\omega_1-\omega_4)t}$ in Equation (21)) and to speed-up and dynamical beats (the sum over n, which reflects the multiple scattering, as has been discussed above).

Reference [24] gives a detailed analysis of synchrotron radiation problem. Both the elastic and inelastic channels are treated in depth according to the coherent-path model.

4. Enhanced-resolution resonant-detector Mössbauer spectroscopy

As will be seen in this section, the coherent-path model can be used to predict the enhanced resolution capability of Mössbauer spectroscopy when using a resonant detector. The result of the analysis will show that, by using a resonant detector in Mössbauer spectroscopy, the spectral line width can be as small as 1.46Γ, where Γ is the line width of the excited-state nuclear level. As is well known, the minimum line width obtained in conventional Mössbauer experiments is 2Γ. The coherent-path model is applied here to a model system consisting of a source nucleus, an absorber nucleus, and the resonant-detector nucleus. This corresponds to the case of a thin absorber [25]. A more general treatment is found in [26]. As noted, the minimum line width obtained in a Mössbauer spectrum taken under

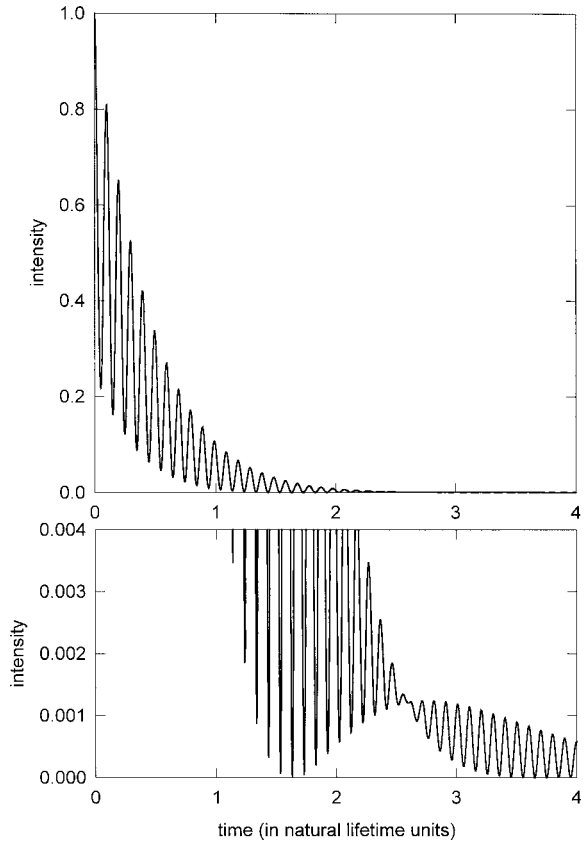

Figure 4. Calculated results for the iron foil case when the magnetic field is in the direction of the synchrotron-radiation beam. Lines 1 and 4 have the same polarization. Lines 3 and 6 also have the same polarization but different from that of lines 1 and 4. In the absence of an electric field gradient at the ^{57}Fe nuclei, there is only one beat pattern corresponding to a beat period of about 14 ns. These results are for the case when the effective number of resonant nuclei is $N = 45$. The lower portion of the figure shows, on an expanded scale, the rather complicated structure in detail.

these conditions is found to be appreciably smaller than the line width obtained in a conventional Mössbauer set-up. Thus the conversion-electron resonant-detector scheme may be used to advantage in experiments requiring the highest possible energy resolution.

A conventional Mössbauer-effect apparatus [27] consists of a radioactive source, an absorber containing the same type of nuclei in the ground state, and a radiation detector such as a proportional counter. One measures the transmitted gamma radiation as a function of the relative velocity of the source with respect to the absorber. The difference, between the proposed experimental set-up and a conventional Mössbauer set-up, is due to the nature of the detector. Instead of a conventional radiation detector, such as a proportional counter or a NaI detector, one

uses a nuclear "resonant" detector. The resonant detector contains ground-state nuclei, which are in resonance with the stationary excited-state source nuclei. In this experimental configuration the absorber is moved with respect to the source and the detector which are both stationary. The experiment proceeds by detecting the conversion electrons generated in the resonant detector as a function of the velocity of the absorber.

Consider a system whose initial condition is as follows. There is: an excited nucleus, having energy $\hbar\omega_0$, at the origin of a coordinate system, an absorber nucleus, whose excited-state energy is $\hbar\omega_0'$, in the ground state (nucleus 1) situated at position x_1, and another ground-state nucleus, having an excited-state energy $\hbar\omega_0$, at position x_2 (nucleus 2). The last nucleus, nucleus 2, represents the resonant detector. The absorber nucleus is situated between the source nucleus and the resonant-detector nucleus. The evolution of the quantum system composed of the three nuclei, the radiation field and the conversion electrons will be investigated below. In the following, the recoilless fractions for emission and absorption are set equal to one for convenience.

One can apply the same mathematical formalism to this system as developed in Section 2. The following amplitudes can be defined; $A(\omega)$ is the amplitude corresponding to the source nucleus excited ($\hbar\omega_0$), the other two nuclei in the ground state, and no photons or conversion electrons present; $B_k(\omega)$ is the amplitude corresponding to all nuclei in ground state, a photon of wave number k and energy $\hbar\omega_k$ present, and no conversion electrons present; $C_i(\omega)$ $(i = 1, 2)$ is the amplitude corresponding to nucleus at position x_i excited, all other nuclei in ground state, and no photons or conversion electrons present; $D_p(\omega)$ is the amplitude corresponding to having a conversion electron from the source nucleus present, having momentum p, all nuclei in the ground state, and no photons present; $E_{ip}(\omega)$ is the amplitude corresponding to having a conversion electron from nucleus i $(i = 1, 2)$ present, all nuclei in ground state, and no photons present. Notice the similarity of these amplitudes to those used in Section 2. In fact, the set of coupled linear equations are almost identical. At $t = 0$, only the source nucleus is excited, so we have the following set of coupled equations

$$(\omega - \omega_0 + \mathrm{i}\varepsilon)A(\omega) = 1 + \sum_k \frac{H_k}{\hbar} B_k(\omega) + \sum_p \frac{H_p}{\hbar} D_p(\omega), \tag{22}$$

$$(\omega - \omega_k + \mathrm{i}\varepsilon)B_k(\omega) = \frac{H_k^*}{\hbar} A(\omega) + \frac{H_k^*}{\hbar} \mathrm{e}^{-\mathrm{i}kx_1} C_1(\omega) + \frac{H_k^*}{\hbar} \mathrm{e}^{-\mathrm{i}kx_2} C_2(\omega), \tag{23}$$

$$(\omega - \omega_0' + \mathrm{i}\varepsilon)C_1(\omega) = \sum_k \frac{H_k}{\hbar} \mathrm{e}^{\mathrm{i}kx_1} B_k(\omega) + \sum_p \frac{H_p}{\hbar} \mathrm{e}^{\mathrm{i}px_i/\hbar} E_{1p}(\omega), \tag{24}$$

$$(\omega - \omega_0 + \mathrm{i}\varepsilon)C_2(\omega) = \sum_k \frac{H_k}{\hbar} \mathrm{e}^{\mathrm{i}kx_2} B_k(\omega) + \sum_p \frac{H_p}{\hbar} \mathrm{e}^{\mathrm{i}px_2/\hbar} E_{2p}(\omega), \tag{25}$$

$$(\omega - \omega_p + \mathrm{i}\varepsilon) D_p(\omega) = \frac{H_p^*}{\hbar} A(\omega), \tag{26}$$

$$(\omega - \omega_p + \mathrm{i}\varepsilon) E_{ip}(\omega) = \frac{H_p^*}{\hbar} \mathrm{e}^{-\mathrm{i}px_i/\hbar} C_i(\omega), \quad i = 1, 2, \tag{27}$$

where all the quantities have been previously defined in one dimension.

One can proceed to solve these equations. After making various substitutions, the resulting summations can be converted to integrals and evaluated using well-known prescriptions [4–6]. In reference [6] the problem corresponding to an initial condition of an excited source nucleus and N resonant absorber nuclei in the ground state has been treated. It has been shown [6] that this problem has a closed-form solution if one restricts the calculation to forward scattering.

The fundamental equation for the source radiation is

$$\left(\omega - \omega_0 + \mathrm{i}\frac{\Gamma}{2\hbar}\right) A(\omega) = 1, \tag{28}$$

where the total width of the excited state Γ is the sum of the conversion-electron and radiative widths

$$\Gamma = \Gamma_c + \Gamma_r. \tag{29}$$

The radiative width in this one-dimensional problem is

$$\Gamma_r = \frac{2L}{\hbar c} \left| H_k(\omega) \right|^2. \tag{30}$$

The simple form of Equation (28) is due to the fact that, when the radiation goes from the source nucleus to one of the ground-state nuclei, it is very unlikely that radiation is re-radiated back to the source nucleus. Macroscopic distances separate the absorber and detector nuclei from the source nucleus thus any such processes are extremely rare. Going back to time domain, it can be easily shown using Equation (28) that

$$a(t) = \mathrm{e}^{-\Gamma t/(2\hbar)}. \tag{31}$$

The source nucleus decays in the normal exponential fashion uninfluenced by the absorber and detector "nuclei". The remaining equations become

$$\left(\omega - \omega_0' + \mathrm{i}\frac{\Gamma}{2\hbar}\right) C_1(\omega) = -\frac{\mathrm{i}\Gamma_r}{2\hbar} \mathrm{e}^{\mathrm{i}(\omega/c)x_1} A(\omega), \tag{32}$$

$$\left(\omega - \omega_0 + \mathrm{i}\frac{\Gamma}{2\hbar}\right) C_2(\omega) = -\frac{\mathrm{i}\Gamma_r}{2\hbar} \mathrm{e}^{\mathrm{i}(\omega/c)x_2} A(\omega) - \frac{\mathrm{i}\Gamma_r}{2\hbar} \mathrm{e}^{\mathrm{i}(\omega/c)(x_2 - x_1)} C_1(\omega). \tag{33}$$

The physical reason why Equation (32) is different from Equation (33) is due to the locations of the absorber nucleus and the detector nucleus relative to the source

nucleus. The radiation coming from the detector nucleus, which is "downstream" with respect to the positive direction of the x-axis from the absorber nucleus, does not "return" to re-excite the absorber nucleus. The conclusion of a careful analysis shows that only radiation coming from nuclei "upstream" from a given nucleus can give a contribution to the excitation of that nucleus, i.e., the radiation effectively only goes forward. When considering an absorber having many nuclei, the same conclusion holds [6]. The fact, noted above, that radiation coming from the absorber nuclei does not get back to the source nucleus is consistent with this conclusion.

Summarizing the results gives

$$A(\omega) = \frac{1}{\omega - \omega_0 + \mathrm{i}\Gamma/(2\hbar)}, \tag{34}$$

$$C_1(\omega) = -\frac{\mathrm{i}\Gamma_r}{2\hbar}\frac{1}{\omega - \omega_0' + \mathrm{i}\Gamma/(2\hbar)}\mathrm{e}^{\mathrm{i}(\omega/c)x_1}A(\omega), \tag{35}$$

$$\begin{aligned} C_2(\omega) \;=\; & -\frac{\mathrm{i}\Gamma_r}{2\hbar}\frac{1}{\omega - \omega_0 + \mathrm{i}\Gamma/(2\hbar)}\mathrm{e}^{\mathrm{i}(\omega/c)x_2}A(\omega) \\ & -\frac{\mathrm{i}\Gamma_r}{2\hbar}\frac{1}{\omega - \omega_0 + \mathrm{i}\Gamma/(2\hbar)}\mathrm{e}^{\mathrm{i}(\omega/c)(x_2-x_1)}C_1(\omega). \end{aligned} \tag{36}$$

Substituting (34) and (35) into (36) gives

$$C_2(\omega) = -\frac{\mathrm{i}\Gamma_r}{2\hbar}\frac{1}{(\omega - \omega_0 + \mathrm{i}\Gamma/(2\hbar))^2}\mathrm{e}^{\mathrm{i}(\omega/c)x_2}\left[1 - \frac{\mathrm{i}\Gamma_r}{2\hbar}\frac{1}{\omega - \omega_0' + \mathrm{i}\Gamma/(2\hbar)}\right]. \tag{37}$$

The probability of having nucleus 2, the "detector nucleus", excited is found from Equation (37).

$$\begin{aligned} \left|C_2(\omega)\right|^2 = & \frac{\Gamma_r^2}{4\hbar^2}\frac{1}{[(\omega - \omega_0)^2 + \Gamma^2/(4\hbar^2)]^2} \\ & + \frac{\Gamma_r^3(\Gamma_r - 2\Gamma)}{16\hbar^4}\frac{1}{[(\omega - \omega_0)^2 + \Gamma^2/(4\hbar^2)]^2}\frac{1}{[(\omega - \omega_0')^2 + \Gamma^2/(4\hbar^2)]}. \end{aligned} \tag{38}$$

The probability of having a conversion electron produced in the "detector" is

$$\begin{aligned} \int_{-\infty}^{+\infty} |C_2(\omega)|^2 \,\mathrm{d}\omega = & \frac{\Gamma_r^2}{4\hbar^2}\int_{-\infty}^{+\infty}\frac{1}{[(\omega - \omega_0)^2 + \Gamma^2/(4\hbar^2)]^2}\mathrm{d}\omega \\ & + \frac{\Gamma_r^3(\Gamma_r - 2\Gamma)}{16\hbar^4}\int_{-\infty}^{+\infty}\frac{1}{[(\omega - \omega_0)^2 + \Gamma^2/(4\hbar^2)]^2} \\ & \times \frac{1}{[(\omega - \omega_0')^2 + \Gamma^2/(4\hbar^2)]}\mathrm{d}\omega. \end{aligned} \tag{39}$$

The first integral is a standard integral. One finds for the first integral a constant value $\pi\hbar\Gamma_r^2/\Gamma^3$. This constant value does not depend on ω_0', the frequency corresponding to the absorber nucleus. This contribution corresponds to the conversion-electron production due to radiation coming directly from the source to the detector nucleus without interacting with the absorber. In the recorded spectrum this will give a constant background analogous to the background observed in a conventional Mössbauer experimental result. The second integral, which will be denoted $I(\omega_0, \omega_0')$, can be calculated by means of contour integration. One finds

$$I(\omega_0, \omega_0') = \frac{\pi\Gamma_r^3(\Gamma_r - 2\Gamma)}{4\hbar\Gamma^3}\frac{12a^2 + \Delta\omega_0^2}{(4a^2 + \Delta\omega_0^2)^2}, \tag{40}$$

where a and $\Delta\omega_0$ are defined as

$$a = \frac{\Gamma}{2\hbar}, \tag{41}$$

$$\Delta\omega_0 = \omega_0 - \omega_0'. \tag{42}$$

Equation (40) gives the conversion-electron distribution as a function of the relative frequency of the absorber nucleus relative to the source (and resonant detector) nucleus. This distribution looks like a Lorentzian, although it is not a real one. The full width at half maximum of this distribution can be calculated easily. One finds a value 1.463Γ. This value is close to 1.47Γ, advanced in [28], where a heuristic approach has been given based on the calculation of the transmission integral. Also in [28], experiments are presented where this narrowing was confirmed using ^{119}Sn. More recently, this narrowing has been observed [29] again with ^{119}Sn.

In order to check the consistency of the model, one can calculate the resulting line width in a conventional Mössbauer procedure using this approach. To do this, consider only the source and absorber nucleus. Then imagine doing the conventional experiment by detecting the conversion electrons produced in the absorber as a function of ω_0'. The result is obtained by solving Equation (32) for $C_1(\omega)$, finding the absolute value squared and integrating over ω, as done above for $C_2(\omega)$. The full width at half maximum is found to be 2Γ as expected.

The results of this section are as follows. The coherent-path model has been applied to a particular type of Mössbauer-effect set-up that makes use of a conventional source, a conventional absorber and a resonant detector consisting of ground-state nuclei with the same environment as the source nuclei. The equations for the complete system of resonant nuclei, gamma radiation, and conversion electrons have been solved. When counting conversion electrons, produced by the resonant detector nuclei, as a function of the Doppler velocity of the absorber with respect to the source and resonant detector, the minimum line width is 1.463Γ. This line width is appreciably less than the minimum line width of 2Γ obtained in a conventional Mössbauer-effect experiment. Thus, for those experiments that

profit from obtaining the highest possible energy resolution, the proposed experimental configuration can be used to advantage. The theory can be extended to the case where both the absorber and detector have an arbitrary thickness. Under such conditions, line broadening will naturally occur, as in conventional Mössbauer spectroscopy, but the advantage of relatively narrower lines, compared to the conventional set-up, will remain.

5. The gamma echo: π phase-shift induced transparency

In the gamma-echo technique the time-differential Mössbauer spectroscopy (TDMS) method is applied. However, in this case the radioactive source is moved, with respect to a nuclear-resonant absorber, during the lifetime of first-excited nuclear state. This introduces a phase shift between the source radiation and the radiation from the absorber. If the source is moved abruptly, introducing a π-phase-shift, the time-dependent intensity shows a sharp increase in the intensity at that time, the "gamma echo". Using the coherent-path model, the gamma-echo effect is seen to be a phase-shift-induced transparency. A closed-form solution for the time-dependent transmitted intensity has been obtained. The solution has the form of a sum over coherent paths that the radiation takes in going from the radioactive source through the absorber to the detector. The model shows that the sharp increase in the intensity, the "gamma-echo", at the time when the source is moved abruptly is due to constructive interference, starting at that time, between the source radiation and the radiation from the absorber. The exact form of the gamma-echo spectrum depends on the movement of the source. Shapes having multiple peaks are possible.

Soon after Rudolph Mössbauer discovered the recoil-free emission and absorption of gamma radiation, the Mössbauer effect was applied to many branches of physics. In fact TDMS experiments were done in 1960–70's and a number of interesting results were obtained [3, 30–33]. Starting in the 1980's a number of more complicated experiments [34–37] were performed based on modifications of the TDMS technique. The "gamma-echo" effect [36, 37] was observed in the early 1990's. All of the above mentioned experiments were analyzed using the semi-classical optical model [3, 23, 38–40] originally due to Hamermesh. More recently a generalization of the semi-classical optical model, using space–time theory [41], has been developed to address the nuclear resonant forward scattering problem.

The semi-classical optical model has proven to be very useful. However, the model does not usually provide a clear physical explanation of the phenomenon being studied. This perhaps explains why the Finnish group [36, 37] coined the term "gamma echo" although they were quite aware that the "gamma echo" was an interference effect. It is not at all clear that there is an "echo" involved in these experiments. The coherent-path model provides a clear physical explanation of the "gamma-echo" phenomenon as simply due to constructive interference between coherent amplitudes.

In order to start on the "gamma-echo" problem, consider the standard TDMS experiment as done in Section 2. Assume the source and absorber nuclear transitions have a single frequency and they are in exact resonance. Then, if the scattering is forward, the time-dependent amplitude for recoil-free radiation reaching the detector according to the coherent-path model is given by Equation (11) above. If all the numerical factors are now included in Equation (11) one finds

$$amp_{\text{recoil-free}}(t) = \sqrt{\frac{f_s\Gamma_r}{2\hbar}}\mathrm{e}^{-\Gamma/(2\hbar)t}\,\mathrm{e}^{-\mathrm{i}\omega_0 t}\left[1+\sum_{n=1}^{N}\binom{N}{n}\left(\frac{-f_a\Gamma_r t}{2\hbar}\right)^n\frac{1}{n!}\right], \quad (43)$$

where all the factors have been previously defined except; f_s which is the recoil-free fraction in the source, and f_a which is the recoil-free fraction in the absorber.

As indicated above, the gamma echo is produced using a TDMS technique in which the source is moved during the lifetime of the first-excited nuclear state. In the pioneering work of the Finnish group [36, 37] a number of different cases of source modulation were presented. Of course there are an infinite number of possibilities. For the purposes of this paper, only the simple idealized case will be considered where the source is moved instantaneously to a new position. A more general treatment of this problem is found in [42].

Assume that the instantaneous source displacement moves the source a distance equal to one-half of the wavelength of the source radiation. It will be seen below that this causes the gamma echo to be a maximum. The wavelength of the radiation from the 14.4 keV transition is 0.086 nm. So now assume that at some instant of time, after time $t = 0$ during the decay of the source, the phase of the source radiation is changed by π. This corresponds to a change in the optical path length, from the source to the detector, by $1/2$ the wavelength. To include this source modulation, we need to incorporate the new situation into our coherent-path model.

The condition, that the phase of the source radiation is instantaneously changed by π at a time $t = t_{\text{switch}}$, can be treated by introducing two amplitudes. The first amplitude corresponds to the source radiating up to time t_{switch} and then changing phase. So this can be written as

$$amp1(t) = \sqrt{\frac{f_s\Gamma_r}{2\hbar}}\mathrm{e}^{-\Gamma/(2\hbar)t}\,\mathrm{e}^{-\mathrm{i}\omega_0 t} \times\left[1-\Phi(t-t_{\text{switch}})+\sum_{n=1}^{N}\binom{N}{n}\left(\frac{-f_a\Gamma_r t}{2\hbar}\right)^n\frac{1}{n!}\right]. \quad (44)$$

Here $\Phi(t - t_{\text{switch}})$ is the Heaviside step function that is 0 for $t < t_{\text{switch}}$ and 1 for $t > t_{\text{switch}}$. Thus $amp1(t)$ corresponds to the usual TDMS situation up to time t_{switch} when the source changes phase. The absorber continues to radiate due to its excitation by the source from time $t = 0$.

The second amplitude corresponds to the situation when the source continues radiating at time t_{switch} but now the radiation has a π phase shift. The second

amplitude is given by

$$amp2(t) = \sqrt{\frac{f_s \Gamma_r}{2\hbar}}\, \mathrm{e}^{-\Gamma/(2\hbar)t} \mathrm{e}^{-\mathrm{i}\omega_0 t} \Theta(t - t_{\mathrm{switch}})\, \mathrm{e}^{\mathrm{i}\pi} \times \left[1 + \sum_{n=1}^{N} \binom{N}{n} \left(\frac{-f_a \Gamma_r (t - t_{\mathrm{switch}}}{2\hbar} \right)^n \frac{1}{n!} \right]. \tag{45}$$

For this second amplitude the source has decayed to its value at time t_{switch} and continues radiating. However, the source radiation amplitude has now acquired a negative value at that time. Also the absorber continues to be excited starting from time t_{switch}. It is the interference between these two amplitudes that gives rise to the "gamma-echo" effect. In order to calculate the final time-dependent intensity, one adds the two amplitudes and then takes the absolute value squared.

$$I_{\pi \text{ phase shift}}(t) = |amp1(t) + amp2(t)|^2. \tag{46}$$

Figure 5 shows the two calculated amplitudes for the ^{57}Fe case when the size of the phase shift is π. The lifetime of the nuclear first-excited state of ^{57}Fe is 141 ns. The nuclear-resonant absorber is characterized by the thickness parameter $\beta = 16$ which corresponds to $N = 98$ in the coherent-path model. The time of the phase shift is fixed at 100 ns. Notice that, in Figure 5, $amp1(t)$ shows the usual initial speed-up and then at $t = t_{\mathrm{switch}}$ the amplitude jumps to a large negative value. This is because the source amplitude is no longer canceling the amplitude of the absorber radiation. As the source continues to radiate from time t_{switch} the amplitude has a negative value and the absorber continues to be excited. Thus

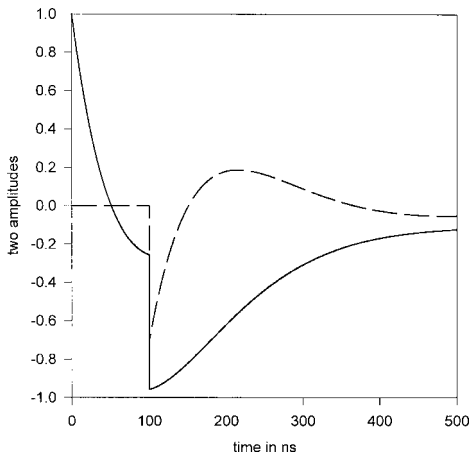

Figure 5. The two amplitudes are shown corresponding to the case when the source is moved instantaneously a distance of 1/2 of the radiation wavelength. The solid curve is $amp1(t)$ and the dashed curve shows $amp2(t)$. Notice how the phase of $amp1(t)$, just after the source is moved, is the same as that of $amp2(t)$. These two amplitudes must be added to obtain the final result.

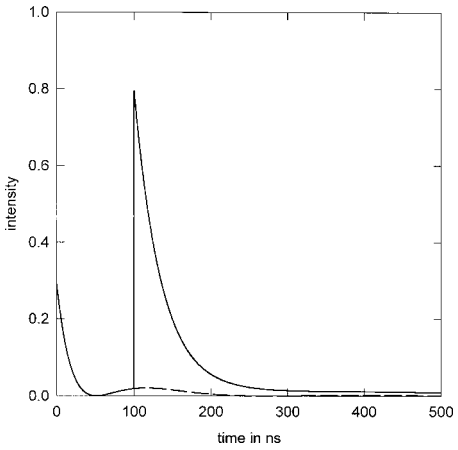

Figure 6. The solid curve shows the "gamma-echo" spectrum. The dashed curve shows the result in the absence of the instantaneous π phase shift of the source. The two curves agree up to the time of the phase shift. Notice the increased area under the gamma-echo spectrum compared with the spectrum without the phase shift. The π phase shift causes the absorber to appear to be somewhat transparent.

$amp2(t)$ has the form of a normal TDMS shape, starting at time t_{switch}, but now with a negative value. It is clear that, when one sums the two amplitudes and takes the absolute value squared to obtain the intensity, there is a large peak at time t_{switch}. This is shown in Figure 6. Figure 6 shows the gamma-echo spectrum and the ordinary TDMS spectrum for comparison.

6. Summary and conclusions

A relatively new field of research is emerging called quantum nucleonic. It deals with coherence and interference effects using resonant gamma radiation. The plan of such research is to approach the success achieved by quantum electronics in the atomic physics field. The ultimate goal would be the development of a gamma-ray laser. In order to succeed one needs to understand nuclear resonant gamma-ray processes as completely as possible. The development of the coherent-path model for nuclear resonant scattering allows one to view nuclear resonant gamma phenomena from a very different point of view. This may provide some new insight that will prove helpful in the development of quantum nucleonics.

The coherent-path model provides a mechanism for understanding the interaction of recoil-free gamma radiation with nuclear resonant matter. The model is so physically transparent that it is easy to understand the main features of nuclear resonant scattering and to apply the theory to new situations, as done here for time-differential Mössbauer spectroscopy, time-differential synchrotron radiation spectroscopy, enhanced-resolution resonant-detector Mössbauer spectroscopy, and the "gamma echo". It is seen that the well-known features, the "speed-up" and

"dynamical-beat" effects, are due to the destructive and constructive interference between coherent amplitudes. The amplitudes that must be summed over correspond to all the indistinguishable paths the recoil-free radiation takes in going from the source through the absorber to the detector. In the theory each path is labeled by the number of effective absorber nuclei encountered in the forward-scattering path. The number of ways each path can occur is given by the appropriate binomial coefficient, which then weights each path. To simplify the language, we describe the multiple recoil-free scattering processes as "hopping" processes. So, for example, the "no-hop" process corresponds to the path when the radiation goes directly from a source nucleus to the detector. For the "one-hop" path, the source radiation interacts with only one effective nucleus. All multiple hopping paths must be considered. The single most important result of the theory is the fact that the odd-numbered-hop amplitudes are 180° out of phase with respect to the source radiation, while the even-numbered-hop amplitudes are in phase with the source radiation. It is interesting to note that, according to the model, it is the one-hop amplitude that is responsible for most of the absorption of radiation by an absorber.

Using the coherent-path model, it has been shown that the energy resolution in Mössbauer spectroscopy experiments can be improved by using the resonant-detector method. Instead of the usual limiting line width of 2Γ, the limiting line width, using the resonant-detector technique, is 1.46Γ.

The coherent-path model can also explain the "gamma-echo" effect in terms that are physically understandable. The phenomenon is simply due to the constructive interference of coherent amplitudes. With this new interpretation we see that there is no "echo". In this paper only one type of source modulation has been considered. If the source displacement is applied instantaneously, one can draw the following conclusions. The closer to $t = 0$ the displacement occurs, the larger the size of the gamma-echo peak. The size of the gamma-echo peak is greatest for a source displacement that corresponds to a π phase shift in the emitted radiation. This is because the phase of the source-radiation amplitude, after the phase shift, is in phase with the amplitude of the radiation coming from the absorber that was excited previously at $t = 0$. An interesting observation in the "gamma-echo" technique is that by applying a π phase shift to the source radiation, early in the decay of the source, one can recover a large portion of the radiation that is incident on the absorber. Thus the absorber appears to be almost transparent. So instead of speaking of a gamma echo, one can say that the phenomenon is due to a π phase-shift-induced transparency.

Using the coherent-path interpretation, which amounts to a sum over indistinguishable paths, it appears that certain recoil-free gamma-ray scattering paths give rise to absorption while others do not. If fact, in the usual transmission experiments, it is the "one-hop" paths that contribute most to absorption, while the "two-hop" paths do not. In the more complicated gamma-echo experiments one can say that, after the π phase shift of the source radiation, the source radiation stimulates the absorber to radiate forward. This is a type of self-stimulated emission. Without

the π phase shift of the source radiation, absorption clearly takes place and the radiation reaching the detector is greatly reduced.

Acknowledgements

As noted in the footnote, this paper is dedicated to Professor Dr. Romain Coussement who immediately recognized the value of the new model and who has been a major supporter of its development. The author would also like to thank Professor Dr. Jos Odeurs whose expertise and hard work have made much of this research successful.

This work was supported in part by the IAP-program P4-07, financed by the Belgian Federal Office for Scientific, Technical and Cultural Affairs, and by the Fonds voor Wetenschappelijk Onderzoek Vlaanderen.

References

1. Mössbauer, R. L., *Z. Physik* **151** (1958), 124.
2. (See, for example) Hoy, G. R., Mössbauer spectroscopy, In: *Encyclopedia of Physical Science and Technology*, Vol. 10, Academic Press, 1992, pp. 469–483.
3. Lynch, F. J., Holland, R. E. and Hamermesh, M., *Phys. Rev.* **120** (1960), 513.
4. Harris, S. M., *Phys. Rev.* **124** (1961), 1178.
5. Heitler, W., *The Quantum Theory Of Radiation*, 3rd edn, Oxford University Press, 1957, p. 164.
6. Hoy, G. R., *J. Phys. C* **9** (1997), 8749.
7. Smirnov, G. V., *Hyp. Interact.* **97/98** (1996), 551 and references therein.
8. Gerdau, E., Rüffer, R., Winkler, H., Tolksdorf, W., Klages, C. P. and Hannon, J. P., *Phys. Rev. Lett.* **54** (1985), 835.
9. *Hyp. Interact.* Part A **123/124** (1999) and *Hyp. Interact.* Part B **125** (2000), E. Gerdau and H. de Waard, (eds), Baltzer Science Publishers.
10. Hannon, J. P. and Trammell, G. T., *Phys. Rev.* **169** (1968), 315.
11. Hannon, J. P. and Trammell, G. T., *Phys. Rev.* **186** (1969), 306.
12. Trammell, G. T. and Hannon, J. P., *Phys. Rev. B* **18** (1978), 165.
13. Hannon, J. P. and Trammell, G. T., *Physica B* **159** (1989), 161.
14. Hannon, J. P. and Trammell, G. T., In: G. Materlik, C. J. Sparks and K. Fisher (eds), *Resonant Anomalous X-Ray Scattering*, Elsevier, Amsterdam, 1994, p. 565.
15. Afanas'ev, A. M. and Kagan, Yu., *JETP* **21** (1965), 215.
16. Afanas'ev, A. M. and Kagan, Yu., *JETP* **25** (1967), 124.
17. Kagan, Yu., Afanas'ev, A. M. and Perstnev, I. P., *JETP* **27** (1968), 819.
18. Kagan, Yu., Afanas'ev, A. M. and Kohn, V. G., *J. Physics C* **12** (1979), 615.
19. Hastings, J. B., Siddons, D. P., van Bürck, U., Hollatz, R. and Bergmann, U., *Phys. Rev. Lett.* **66** (1991), 770.
20. van Bürck, U., Siddons, D. P., Hastings, J. B., Bergmann, U. and Hollatz, R., *Phys. Rev. B* **46** (1992), 6207.
21. Sturhahn, W. and Gerdau, E., *Phys. Rev. B* **49** (1994), 9285.
22. Kikuta, S., In: G. Materlik, C. J. Sparks and K. Fisher (eds), *Resonant Anomalous X-Ray Scattering*, Elsevier, Amsterdam, 1994, p. 635 and references therein.
23. Hoy, G. R., *Hyp. Interact.* **107** (1997), 381 and unpublished results.
24. Hoy, G. R., Odeurs, J. and Coussement, R., *Phys. Rev. B* **63** (2001), 184 435.
25. Odeurs, J., Hoy, G. R. and L'abbé, C., *J. Phys.: Condens. Matter* **12** (2000), 637.

26. Odeurs, J., Hoy, G. R., L'abbé, C., Shakhmuratov, R. N. and Coussement, R., *Phys. Rev. B* **62** (2000), 6146.
27. Greenwood, N. N. and Gibb, T. C., *Mössbauer Spectroscopy*, Chapman and Hall, London, 1971.
28. Mitrofanov, K. P., Illarionova, N. V. and Shpinel, Y. S., *Prib. Tekhn. Eksp.* **30** (1963), 49.
29. Odeurs, J., Hoy, G. R., L'abbé, C., Koops, G. E. J., Pattyn, H., Shakhmuratov, R. N., Coussement, R., Chiodini, N. and Paleari, A., International Symposium on the Industrial Applications of the Mössbauer Effect, ISIAME 2000, submitted for publication.
30. Neuwirth, W., *Z. Phys.* **197** (1966), 473.
31. Triftshauser, W. and Craig, P. P., *Phys. Rev.* **162** (1967), 274.
32. Hamill, D. W. and Hoy, G. R., *Phys. Rev. Lett.* **21** (1968), 724.
33. Hoy, G. R. and Wintersteiner, P. P., *Phys. Rev. Lett.* **28** (1972), 877.
34. Helistö, P., Ikonen, E., Katila, T. and Riski, K., *Phys. Rev. Lett.* **49** (1982), 1209.
35. Shvyd'ko, Yu. V., Smirnov, G. V., Popov, S. L. and Hertrich, T., *Pis'ma Zh. Eks. Teor. Fiz.* **53** (1991), 69 [Engl. transl. *JETP Lett.* **53** (1991), 69].
36. Helistö, P., Tittonen, I., Lippmaa, M. and Katila, T., *Phys. Rev. Lett.* **66** (1991), 2037.
37. Tittonen, I., Lippmaa, M., Helistö, P. and Katila, T., *Phys. Rev. B* **47** (1993), 7840.
38. Perlow, G. J., *Phys. Rev. Lett.* **40** (1978), 896.
39. Monahan, J. E. and Perlow, G. J., *Phys. Rev. A* **20** (1979), 1499.
40. Ikonen, E., Helistö, P., Katila, T. and Riski, K., *Phys. Rev. A* **32** (1985), 2298.
41. Shvyd'ko, Y. V., *Phys. Rev.* **59** (1999), 9132.
42. Hoy, G. R. and Odeurs, J., *Phys. Rev. B* **63** (2001), 64 301.